Spring 5-1-2020

THERMODYNAMIC POTENTIAL OF VERY HIGH PERFORMANCE FUEL CELLS

Kimberly Liang
kimberly.liang@uconn.edu

UCONN
SCHOOL OF ENGINEERING
MECHANICAL ENGINEERING

THERMODYNAMIC POTENTIAL OF VERY HIGH PERFORMANCE FUEL CELLS

Kimberly Liang

Honors Major: Mechanical Engineering

Thesis Advisor: Dr. Ugur Pasaogullari

Honors Advisor: Dr. Jason Lee

THESIS
MAY 2020

I. Executive Summary

Fuel Cells are devices that use the chemical energy of a fuel (e.g. hydrogen) to electrochemically produce electricity. Similar to a conventual combustion engine, a fuel cell will continue to run and generate electricity as long as fuel is supplied. However, unlike a conventional combustion engine, fuel cells have a much higher theoretical efficiency and do not directly emit harmful air pollutants. This project will focus on a fuel cell that uses hydrogen as fuel and oxygen as an oxidizing agent.

As fuel cell technology evolved, high pressure fuel cell systems became of interest in portable applications, such as submarine oxygen generation, space station life support, or other places where oxygen is scarce. However, subjecting the fuel cell to such high pressures has had questionable results. Prior research in the field has shown that increasing operating pressure can increase voltage and power density, but can also introduce drawbacks such as increased gas permeation and water management issues.

The objective of this project is to investigate the thermodynamics of fuel cells to determine if there is a significant benefit to running fuel cells at very high pressures. Typically, fuel cells are run between 1-3 atm, but this project deals with pressure up to 160 atm. A thermodynamic model that includes the change in Gibbs free energy with high pressure and resulting thermodynamic potential increase was developed. The model included non-ideal gas behavior to accurately determine the potential benefits of high-pressure operation.

The results show that there are benefits, in terms of thermodynamics, in running hydrogen fuel cell systems at high pressures. However, this model only considers the thermodynamics; there may be other drawbacks that were not investigated.

Table of Contents

II. List of Figures and Tables

III. Project Statement

i. Project Background

This project was completed under the direction of Dr. Ugur Pasaogullari, who currently is the director of UConn's Center for Clean Energy Engineering (C2E2) and a professor in UConn's department of Mechanical Engineering. Since its establishment in 2001, C2E2 has received funding and investment of $14.5 million from Connecticut Clean Energy Fund, the U.S Department of Energy (DOE), and other industry partners such as United Technologies Corporation (or Raytheon Technologies Corporation, as of April 2020), Siemens, General Electric, and Praxair. C2E2 is a hub for multidisciplinary energy research, education, training, and outreach. The faculty, staff, and students at C2E2 strives to develop and validate advanced energy systems to create a global sustainable energy economy.

Fuel Cells development dates back to almost 200 hundred years ago. In the early 1800s, William Nicholson and Anthony Carlisle first described electrolysis.

$$2H_2O_{(l)} \rightarrow 2H_{2\,(g)} + O_{2\,(g)} \quad (1)$$

40 years later, Michael Faraday derived the Laws of Electrolysis:

1. First Law of Electrolysis: The mass of a substance produced at an electrode during electrolysis is proportional to the number of moles of electrons (the quantity of electricity) transferred at that electrode.
2. Second Law of Electrolysis: The number of Faradays of electric charge required to discharge one mole of substance at an electrode is equal to the number of "excess" elementary charges on that ion [1].

These Laws laid the foundation for fuel cells.

In 1838, William Robert Grove was able to reverse the electrolysis process to produce energy.

$$2H_{2\,(g)} + O_{2\,(g)} \rightarrow 2H_2O_{(l)} + energy \quad (2)$$

He did so while performing a series of experiments with two platinum electrodes, sulfuric acid, oxygen, and hydrogen. One end the platinum electrodes were submerged in sulfuric acid, while the other end was submerged in either hydrogen or oxygen. These experiments showed that a steady electric current was produced by the electrochemical reaction between oxygen and hydrogen over a platinum catalyst.

In the 1930s, Francis T. Bacon built upon Grove's experiments by using alkaline electrolytes instead of acid electrolytes and gas-diffusion electrodes instead of solid electrodes, which birthed a new type of fuel cell, the alkaline fuel cell (AFC).

Bacon's AFC found popularity at the beginning of the Space Race in the late 1950s and early 1960s, where NASA began utilizing fuel cells for manned space missions. UTC Power and Pratt & Whitney assembled AFCs for the Apollo missions, where the water by-product was used as drinking water for astronauts. In the mid-1960s, a General Electric (GE) researchers Willard Thomas Grubb and Leonard Niedrach developed Proton Exchange Membrane Fuel Cells (PEMFC), which were used on NASA's Gemini missions.

In the 1970s, the US began extremely dependent on imported oil, resulting in members of the Organization of Arab Petroleum Exporting Countries (OAPEC) imposing an oil embargo on the US and other western countries. At the same time, Americans became increasingly concerned about climate change. This pushed the community to develop more alternative energy technologies, which resulted in heightened popularity of Phosphoric Acid Fuel Cells (PAFC).

Originally developed in 1961 by Elmore and Tamer, PAFCs used a new electrolyte made of phosphoric acid and silica powder and ran on air instead of oxygen.

In the 1990s, Solid Oxide Fuel Cells (SOFCs) and PEMFCs became the focus of field due to their potential commercialization for small stationary applications. Also around this time, Molten Carbonate Fuel Cells (MCFCs) gained popularity for large stationary applications.

Finally, in the 2000s, fuel cells continue to be a popular research interest due to heightened concerns of energy security. Large auto manufacturers such as Hyundai, Toyota, and Honda have released fuel cell cars for civilian use, and Exxon Mobil began a partnership with FuelCell Energy in 2019 to develop fuel cell technologies for capturing carbon dioxide from industrial facilities [2].

ii. Problem Definition

The objective of this project is to investigate the thermodynamics of a PEMFC as it approaches very high pressures. Specifically, this project models the relationship between Gibbs Free Energy and equilibrium potential versus pressures from 0.1 to 160 atm. Since the domain of this model deviates from ideal gas assumptions, fugacity must also be included in these calculations.

iii. Technical Specifications

Units: SI (Kelvin, Amps, seconds, Joules, moles, atm)

Data analysis: MATLAB

IV. Theory

Fuel cells with H+ as its charge carrier can be either a Proton Exchange Membrane Fuel Cell (PEMFC) or Phosphoric Acid Fuel Cell (PAFC). However, since PAFCs cannot operate at high pressures, the model will focus on PEMFCs. The reaction that occurs in the anode is:

$$H_2 \rightarrow 2H^+ + 2e^- \quad (2)$$

The cathode:

$$\frac{1}{2}O_2 + 2H^+ + 2e^- \rightarrow H_2O \quad (3)$$

And the overall reaction:

$$H_2 + \frac{1}{2}O_2 \rightarrow H_2O \quad (4)$$

The oxidation half-cell reaction or hydrogen oxidation reaction (HOR) occurs at the anode. The reduction half-cell reaction or oxygen reduction reaction (ORR) occurs at the cathode.

A general diagram of PAFCs and PEMFCs are shown in Figures 1 and 2, respectively. Both types of fuel cells follow the same process. Fuel is fed into the anode, where hydrogen is oxidized, as described in Equation 2. Electrons, one of the products from Equation 2, travel through an external circuit, creating electric current. The other product from Equation 2, H+, travels across the membrane to the cathode, to complete the reduction of oxygen from the air that was fed into the cell, as described in Equation 3. Then, excess fuel is expelled on the anode side while excess water, heat, or gas are expelled on the cathode side. Though PAFCs and PEMFCs have different membranes between the anode and cathode, the basic electrochemical reactions are the same.

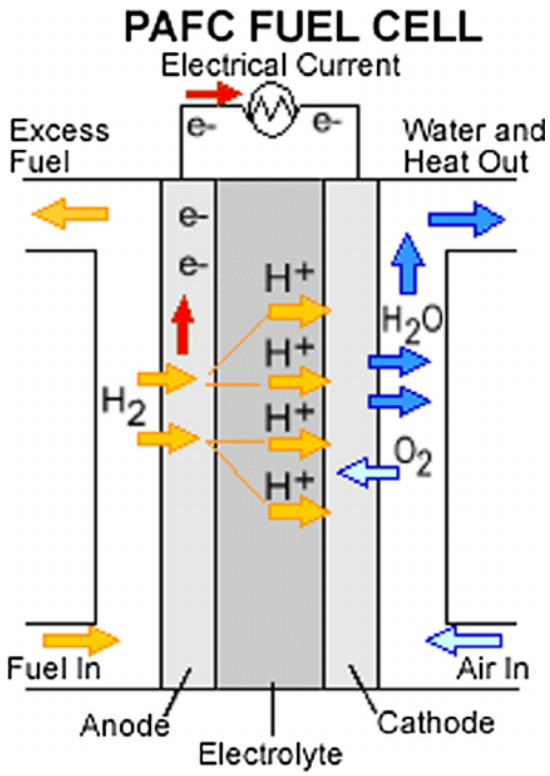

Figure 1: Schematic of Phosphoric Acid Fuel Cell (PAFC) [3]

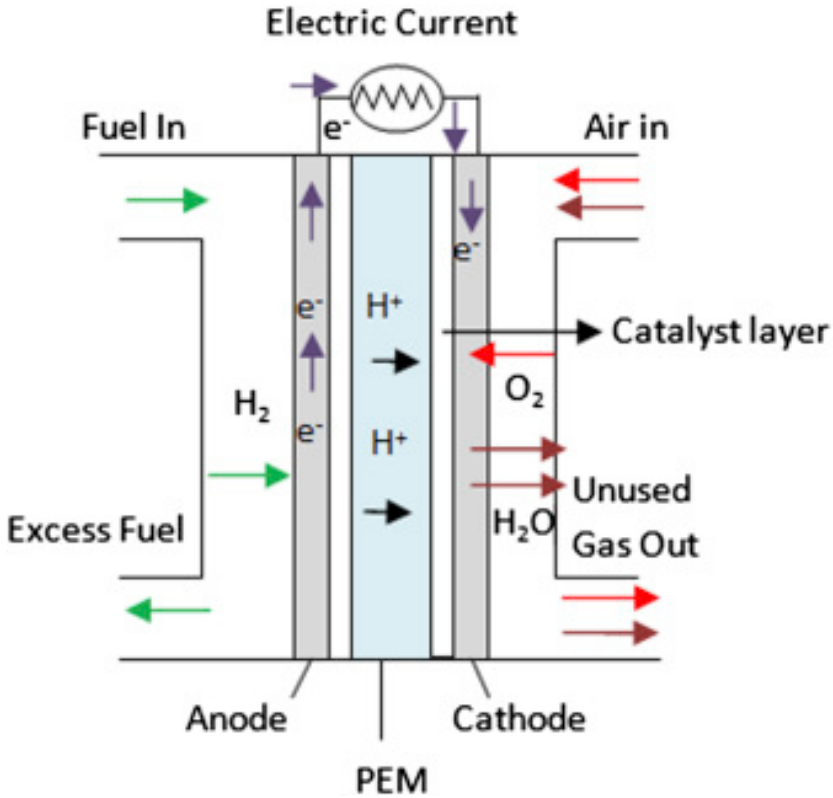

Figure 2: Schematic of Proton Exchange Membrane Fuel Cell (PEMFC) [4]

The chemical potential of an ideal gas is:

$$\mu_i^{ig} = G_i^{ig} + RTlny_i \tag{5}$$

Where μ_i^{ig} is the chemical potential for an ideal gas, R is the ideal gas constant, and G_i^{ig} is the initial Gibbs energy for an ideal gas.

The definition of Gibbs Free Energy is:

$$G \equiv H - TS \tag{6}$$

Where G is the Gibbs energy, H is enthalpy, T is temperature, and S is entropy. Assuming one mole of a homogeneous fluid of constant compression, this becomes

$$dG = VdP - SdT \tag{7}$$

Where V is volume. At constant T for an ideal gas, this becomes

$$dG_i^{ig} = VdP = \frac{RT}{P}dP = RTdlnP \tag{8}$$

Integration yields:

$$G_i^{ig} = \Gamma_i(T) + RTlnP \tag{9}$$

Where Γ_i is the integration constant dependent on temperature.

Thus, Eqn. (5) can be rewritten as

$$\mu_i^{ig} = \Gamma_i(T) + RTlny_iP \tag{10}$$

For a real gas, the analogous equation to equation 8 is

$$G_i = \Gamma(T) + RTlnf \tag{11}$$

Where f is fugacity, and G_i is the initial Gibbs Free Energy for a real gas. Thus, to find the change in Gibbs Free energy, we subtract Eqn. (9) from Eqn. (11) to find

$$G_i - G_i^{ig} = RTln(\frac{f}{P}) \tag{12}$$

The ratio $\frac{f}{P}$ is the fugacity coefficient, Φ.

To use Equation 10, the definition of Φ was used to calculate the fugacities for hydrogen and oxygen at 14 different pressures (i.e. 0.1, 0.5, 1, 2, 5, 10, 20, 40, 60, 80, 100, 120, 140, and 160 atm). Assuming the water activity remains constant at 1 and using the balanced chemical equations in equation 4, equation 10 becomes

$$G_i = G_i^{ig} - RTln\left[f_{H_2}(f_{O_2})^{1/2}\right] \tag{13}$$

The Nernst equation for an ideal gas is:

$$E = E^o + \frac{RT}{nF} lnQ \tag{14}$$

Where E is the cell potential, E^o is the standard cell potential, R is the universal gas constant, T is temperature, and Q is the reaction quotient. At time t, the reaction quotient is:

$$Q(t) = \frac{\Pi_i^{products} a_i^{v_i}}{\Pi_j^{reactants} a_j^{v_j}} \tag{15}$$

Where $Q(t)$ is the reaction quotient at time t, a_i is the activity of each product raised to its corresponding reaction coefficient, v_i. Similarly, a_j is the activity of each reactant raised to its corresponding reaction coefficient, v_j. For real gasses, the activity is effective partial pressure, or fugacity. Thus, assuming the water activity remains constant at 1, Eqn. (14) becomes

$$E = E^o + \frac{RT}{nF} ln[f_{H_2}(f_{O_2})^{1/2}] \tag{16}$$

Because of fugacity, the change in Gibbs free energy and cell potential will be greater than if it was an ideal gas.

Consequently, fugacity will affect the change in entropy. Change in entropy is defined as:

$$\Delta s = \int_{T_1}^{T_2} \frac{C_p}{T} dT - R \int_{P_1}^{P_2} dP \tag{17}$$

Assuming constant specific heats, this simplifies to:

$$\Delta s = C_p \ln \left(\frac{T_2}{T_1}\right) - Rln\left(\frac{p_2}{p_1}\right) \tag{18}$$

Replacing the pressures with fugacity, this will become

$$\Delta s = C_p \ln\left(\frac{T_2}{T_1}\right) - Rln\left(\frac{f_2}{f_1}\right) \quad (19)$$

Finally, the thermodynamic potential was found at three different temperatures (i.e. 300, 500, and 800 K), so the corresponding specific heat capacities for each temperature were also calculated using Shomate's equation, which is as follows:

$$C_P = A + Bt + Ct^2 + Dt^3 + \frac{E}{t^2} \quad (20)$$

Where C_P is the specific heat capacity at constant pressure, A, B, C, D, and E are coefficients that depend on the gas, and t is the temperature divided by 1000. The coefficients used are included in the appendix.

V. Results

i. MATLAB Code

a. Definitions

```
F = 96485.3329; %Faraday's number, C/mol R = 8.314; %J/(mol*K)
To = 300; %K
T_std = 298.15; %K

n = 2;
```

b. Defining pressures and fugacity

```
p = [0.1, 0.5, 1, 2, 5, 10, 20, 40, 60, 80, 100, 120, 140, 160]; %pressure,
atm

% phi = f/p

% 300 K

phi_H2_300 = [1.0005, 1.00026, 1.0053, 1.00105, 1.00264, 1.00532, 1.0108,
1.0221, 1.0340, 1.0464, 1.0592, 1.0728, 1.0866, 1.101]; %fugacity coeff for
hydrogen

phi_O2_300 = [0.99994, 0.99967, 0.99935, 0.99870, 0.99675, 0.99356, 0.9873,
0.9755, 0.965, 0.955, 0.946, 0.937, 0.930, 0.924]; %fugacity coeff for oxygen
```

```
f_H2_300 = p.*phi_H2_300; f_O2_300 = p.*phi_O2_300;

%500 K

phi_H2_500 = [1.00004, 1.00020, 1.00039, 1.00079, 1.00197, 1.00396, 1.00797,
1.01615, 1.0245, 1.0331, 1.0419, 1.0509, 1.0600, 1.069]; %fugacity coeff for
hydrogen

phi_O2_500 = [1.00002, 1.00012, 1.00023, 1.00046, 1.00116, 1.00234, 1.00472,
1.00961, 1.0147, 1.0199, 1.0253, 1.0253, 1.0253, 1.0253]; %fugacity coeff for
oxygen

f_H2_500 = p.*phi_H2_500;

f_O2_500 = p.*phi_O2_500;

%800 K

phi_H2_800 = [1.00003, 1.00014, 1.00027, 1.00055, 1.00137, 1.00274, 1.00551,
1.0111, 1.0168, 1.0225, 1.0284, 1.0343, 1.0403, 1.046];

phi_O2_800 = [1.00004, 1.00018, 1.00036, 1.00071, 1.00179, 1.0036, 1.0072,
1.0144, 1.0216, 1.0288, 1.0361, 1.0435, 1.0508, 1.0582];

f_H2_800 = p.*phi_H2_800; f_O2_800 = p.*phi_O2_800;
```

c. Calculating standard cell potential

LHV, used water vapor values

standard enthalpy values

```
h_H2 = 0;
h_O2 = 0;
h_H2O = -241.98E3; %J/mol h_rxn = h_H2O-(h_H2+0.5*h_O2); h_std = [h_H2 h_O2
h_H2O];

% standard entropy values s_H2 = 130.6; %J/mol*K
s_O2 = 205; %J/mol*K
s_H2O = 188.8; %J/mol*K
s_rxn = s_H2O-(s_H2+0.5*s_O2); s_std = [s_H2 s_O2 s_H2O];

Go = h_rxn+298.15*s_rxn;
```

d. Cp values (Shomate's Equation)

Resulting Cp values are in J/mol*K

```
T = [500 800]; %K
for i = 1:2

t = T./1000;
```

```
        if t(i)<1

              Cp_H2(i) = 33.066178-11.363417.*t(1)+11.432816*t(i).^2-
              2.772874.*t(i).^3-0.158558./ (t(i).^2);

        else

              Cp_H2(i) = 18.563083+12.257357.*t(1)-
              2.859786*t(i).^2+0.268238.*t(i).^3+1.977990./ (t(i).^2);

        end


        if t(i)<0.7

        Cp_O2(i) = 31.32234-20.23531.*t(i)+57.86644.*t(i).^2-36.50624.*t(i).^3-
        0.007374./ (t(i).^2);

        else

        Cp_O2(i) = 30.03235+8.772972.*t(i)-3.988133.*t(i).^2+0.788313.*t(i).^3-
        0.741599./ (t(i).^2);

        end

        Cp_H2O(i) = 30.09200+6.832514.*t(i)+6.793435.*t(i).^2-
        2.534480.*t(i).^3+0.082139./ (t(i).^2);

end

Cp = [Cp_H2; Cp_O2; Cp_H2O];
```

e. Calculating non-standard enthalpy/entropy values

For 500 K

```
h_H2_500 = h_H2+Cp(1,1)*(T(1)-T_std); h_O2_500 = h_O2+Cp(2,1)*(T(1)-T_std);
h_H2O_500 = h_H2O+Cp(3,1)*(T(1)-T_std); h_500 = h_H2O_500-h_H2_500-
0.5*h_O2_500;

s_H2_500 = s_H2+Cp(1,2)*log(T(1)/T_std); s_O2_500 =
s_O2+Cp(2,2)*log(T(1)/T_std); s_H2O_500 = s_H2O+Cp(3,2)*log(T(1)/T_std);
s_500 = s_H2O_500-s_H2_500-0.5*s_O2_500;

G_500 = h_500-500*s_500;

% For 800

h_H2_800 = h_H2+Cp(1,2)*(T(2)-T_std); h_O2_800 = h_O2+Cp(2,2)*(T(2)-T_std);
h_H2O_800 = h_H2O+Cp(3,2)*(T(2)-T_std); h_800 = h_H2O_800-h_H2_800-
0.5*h_O2_800;
```

```
s_H2_800 = s_H2+Cp(1,2)*log(T(2)/T_std); s_O2_800 =
s_O2+Cp(2,2)*log(T(2)/T_std); s_H2O_800 = s_H2O+Cp(3,2)*log(T(2)/T_std);
s_800 = s_H2O_800-s_H2_800-0.5*s_O2_800;

G_800 = h_800-800*s_800;
```

f. Calculating thermodynamic potential

```
E_th = -Go./(n*F);
E_eq = E_th+(R*T_std/(n*F))*log(f_H2_300.*(f_O2_300.^0.5));

E_500 = (-G_500/(n*F))+(R*T(1)/(n*F))*log(f_H2_500.*(f_O2_500.^0.5)); E_800 =
(-G_800/(n*F))+(R*T(2)/(n*F))*log(f_H2_800.*(f_O2_800.^0.5));
```

g. Calculating Gibbs Free Energy

```
delta_G = Go - R.*T_std*log(p.*f_H2_300.*(p.*(f_O2_300).^0.5));
```

h. Plots

```
plot(log(p), delta_G);
title('Gibbs Free Energy vs Pressure (Logarithmic Scale)')
xlabel('log(Pressure) (atm)')
ylabel('Gibbs Free Energy (J/mol)')

figure
plot(p, delta_G);
title('Gibbs Free Energy vs Pressure')
xlabel('log(Pressure) (atm)')
ylabel('Gibbs Free Energy (J/mol)')

figure
plot(p,E_eq)
title('Thermodynamic Potential vs Pressure')
xlabel('Pressure (atm)')
ylabel('Thermodynamic Potential (V)')
hold on
plot(p,E_500)
hold on
plot(p,E_800)
hold off
legend('300K','500K','800K','Location','southeast')

figure
plot(log(p),E_eq)
title('Thermodynamic Potential vs Pressure (Logarithmic Scale)')
xlabel('log(Pressure)(atm)')
ylabel('Thermodynamic Potential (V)')
hold on
plot(p,E_500)
hold on
plot(p,E_800)
hold off
legend('300K','500K','800K','Location','southeast')
```

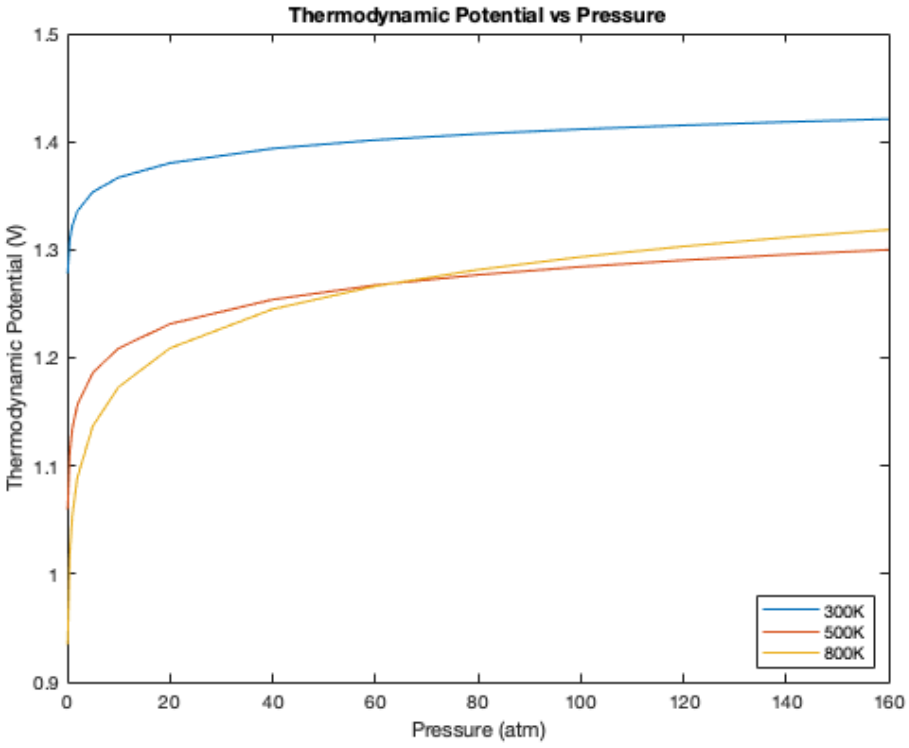

Figure 3: Thermodynamic Potential vs Pressure

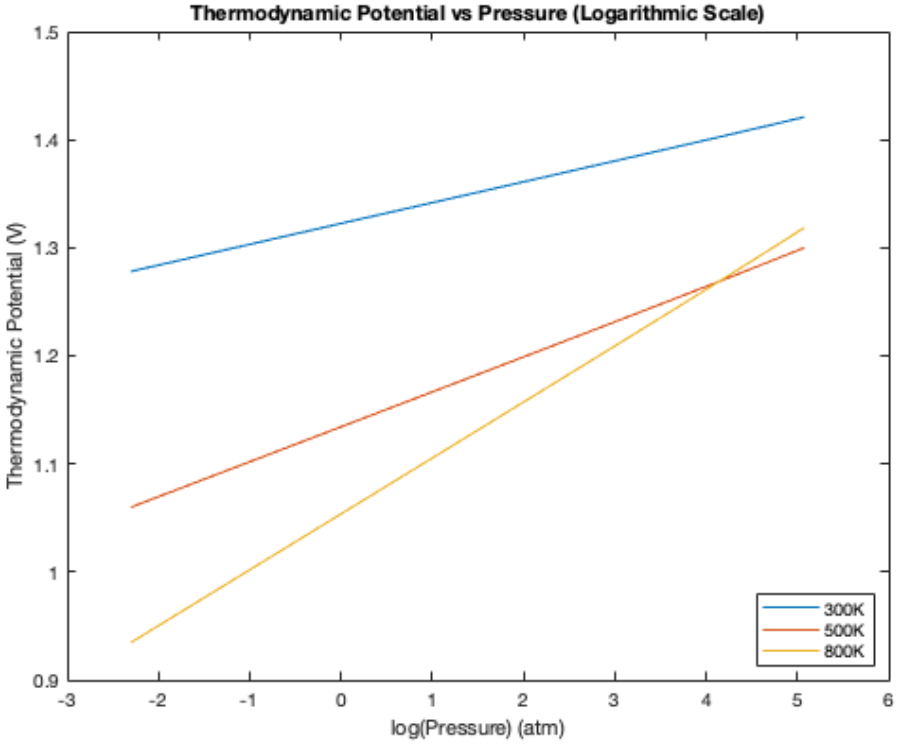

Figure 4: Thermodynamic Potential vs Pressure, Logarithmic Scale

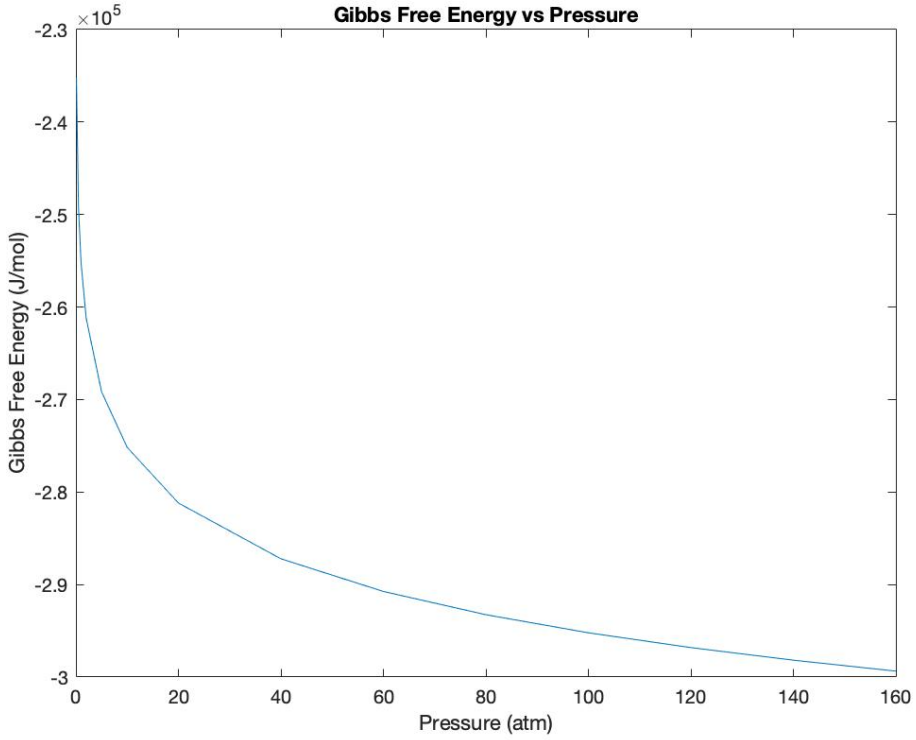

Figure 5: Gibbs Free Energy vs Pressure

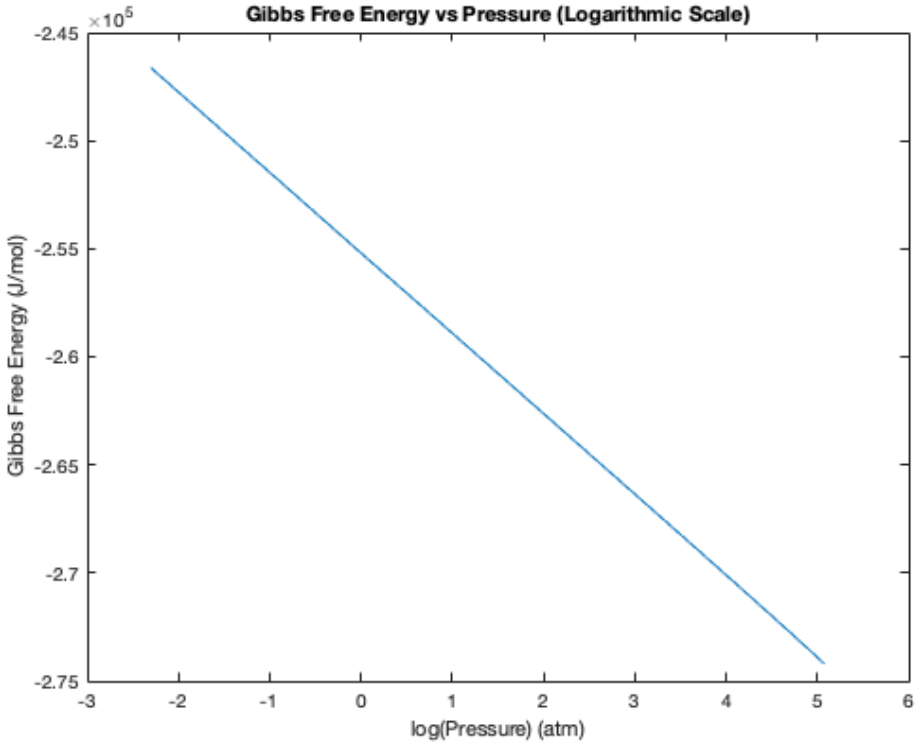

Figure 6: Gibbs Free Energy vs Pressure, Logarithmic Scale

ii. Analysis

Figures 3-6 show the relationships between thermodynamic potential and Gibbs Free Energy versus pressure. As shown in Figures 3 and 4, thermodynamic potential increases with pressure. The final voltages for 300, 500, and 800 K, respectively, are 1.4209, 1.300, and 1.3186 V. Thus, in terms of thermodynamic potential, it is most beneficial to run the fuel around room temperature and at high pressures. Figure 4 shows that Gibbs Free energy decreases as pressure increases. This demonstrates that the reaction is more favorable, more likely to occur, or less external energy is needed for the reaction to occur.

VI. Summary/Conclusions

While the first well-known use of fuel cells was in the aerospace industry, the applications of fuel cells are expanding to other portable applications, some of which require hydrogen and/or oxygen at high pressures. At high pressures, these gases will deviate from ideal gas assumptions, and the fuel cell itself may experience adverse consequences in terms of its operational ability.

The objective of this project was to develop a model to develop and investigate the thermodynamics of very high-pressure fuel cells. A model was constructed in MATLAB to show the relationship between Gibbs free energy and equilibrium cell potential vs pressure. The model included pressures from 0.1 to 160 atm, and calculated the cell potential at three temperatures: 300, 500, and 800 K.

The model shows that cell potential increases with pressure, and the highest voltage is achieved at 300K. The model also shows that Gibbs Free Energy decreases with pressure, meaning that as pressure increases, the more likely the electrochemical reactions are to occur.

However, these results are not conclusive for the entire fuel cell system, since the model only focuses on the thermodynamics of the fuel cell. Future work will include an investigation on the effect of high pressures on the electrolyte membranes and, consequently, water management and gas permeation.

VII. References

[1] E. I. Ortiz-Rivera, A. L. Reyes-Hernandez and R. A. Febo, "Understanding the History of Fuel Cells," *2007 IEEE Conference on the History of Electric Power,* pp. 117-122, 2007.

[2] "ExxonMobil," 6 November 2019. [Online]. Available: https://corporate.exxonmobil.com/News/Newsroom/News-releases/2019/1106_ExxonMobil-and-FuelCell-Energy-expand-agreement-for-carbon-capture-technology.

[3] H. Vaghari, H. Jafarizadeh, A. Berenjian and N. Anarjan, "Recent Advances in Application of Chitosan in Fuel Cells," *Sustainable Chemical Processes,* vol. I, 2013.

[4] V. S. Mohan, S. Varjani and A. Pandey, Microbial Electrochemical Technology: Sustainable Platform for Fuels, Chemicals and Remediation, Elsevier, 2018.

[5] National Institutue of Standards and Technology, U.S. Department of Commerce, "NIST Chemistry WebBook," [Online]. Available: https://webbook.nist.gov/cgi/cbook.cgi?ID=C7782447&Mask=1#Thermo-Gas.

VIII. Appendix

i. Coefficients for Shomate's Equation

Table 1: Coefficients for Shomate's Equation, Oxygen Gas [5]

Temperature (K)	100.-700.	700.-2000.
A	31.32234	30.03235
B	-20.23531	8.772972
C	57.86644	-3.988133
D	-36.50624	0.788313
E	-0.007374	-0.741599

Table 2: Coefficients for Shomate's Equation, Hydrogen Gas [5]

Temperature (K)	298.-1000.
A	33.066178
B	-11.363417
C	11.432816
D	-2.772874
E	-0.158558